Field-driven metamorphoses of isolated skyrmions within the conical state of cubic helimagnets

Leonov, Andrey O.; Pappas, C.; Smalyukh, Ivan I.

DOI
10.1103/PhysRevB.104.064432

Publication date
2021

Document Version
Final published version

Published in
Physical Review B

Field-driven metamorphoses of isolated skyrmions within the conical state of cubic helimagnets

Andrey O. Leonov,[1,2,3,*] C. Pappas,[4,2,†] and Ivan I. Smalyukh[5,6,7,2,‡]

[1]*Department of Chemistry, Faculty of Science, Hiroshima University Kagamiyama, Higashi Hiroshima, Hiroshima 739-8526, Japan*

[2]*Chirality Research Center, Hiroshima University, Higashi Hiroshima, Hiroshima 739-8526, Japan*

[3]*IFW Dresden, Postfach 270016, D-01171 Dresden, Germany*

[4]*Faculty of Applied Sciences, Delft University of Technology, Mekelweg 15, 2629JB Delft, The Netherlands*

[5]*Soft Materials Research Center and Materials Science and Engineering Program, University of Colorado, Boulder, Colorado 80309, USA*

[6]*Department of Physics and Department of Electrical, Computer and Energy Engineering, University of Colorado, Boulder, Colorado 80309, USA*

[7]*Renewable and Sustainable Energy Institute, National Renewable Energy Laboratory and University of Colorado, Boulder, Colorado 80309, USA*

(Received 23 March 2021; revised 1 June 2021; accepted 2 August 2021; published 18 August 2021)

Topologically stable field configurations appear in many fields of physics, from elementary particles to condensed matter and cosmology. Deep physical relations and common physical features of a large variety of very different solitonic states in these systems arise from the mathematical similarity of phenomenological equations. During the last decade, chiral liquid crystals and chiral magnets took on the role of model objects for the experimental investigation of topological solitons and the understanding of their nonsingular field configurations. This is directly related to the discovery of particle-like chiral skyrmions, which are also considered as promising ingredients for technological applications. Here we introduce a paradigm of facile skyrmionic networks with mutually orthogonal orientations of constituent isolated skyrmions. On the one hand, such networks are envisioned as a novel concept of spintronic devices based, e.g., on gapless skyrmion motion along each other, and are presumably responsible for precursor phenomena near the ordering temperatures of bulk cubic helimagnets. In particular, we demonstrate an interconversion between mutually orthogonal skyrmions: horizontal skyrmions may swirl into an intermediate spring-like state and subsequently squeeze into vertical skyrmions with both polarities. On the other hand, skyrmion tubes are considered as building blocks for particle-like states with more involved internal structure. A family of target-skyrmions, which includes a so far overlooked type with a multiple topological charge, is formed owing to the tendency to minimize the interaction energy between vertical and horizontal skyrmions. The conical phase serves as a suitable background for considered skyrmion evolution. It substantializes the attracting skyrmion-skyrmion interaction in the skyrmionic networks, shapes their internal structure, and guides the nucleation processes. Alternatively, intricate textural changes of isolated skyrmions result not only in the structural deformations of a host conical state, but may lead to the formation of an exotic skyrmion order with pairs of merons being the core of the game. Generically, the fundamental insights provided by this work emphasize a three-dimensional character of skyrmion metamorphoses and can also be extended to three-dimensional solitons, such as hopfions.

DOI: 10.1103/PhysRevB.104.064432

I. INTRODUCTION

Multidimensional localized structures (topological defects or localized states) are the focus of research in many fields of modern physics [1,2]. Since the late 1960s, the problem of soliton-like solutions of nonlinear field equations has been addressed in condensed matter physics, biophysics, in particle and nuclear physics, in astrophysics, and cosmology [3]. From a fundamental point of view, the interest in such solutions is related to the explanation of countable particles in continuous fields. Within the structural theory the particle-like properties are ascribed to localized solutions of nonlinear field equations and the physical fields are described by the asymptotic behavior of corresponding solutions. Hobart and Derrick [4], however, found with general arguments that multidimensional localized states are unstable in many physical field models: inhomogeneous states may appear only as dynamic excitations, but static configurations collapse spontaneously into topological singularities. As a consequence, the solutions of corresponding nonlinear field equations are restricted to one-dimensional solitons. The instabilities of localized field configurations can be overcome, if the energy functionals contain, for example, contributions with higher-order spatial derivatives. This original idea of Skyrme in the 1960s succeeded in describing the nuclear particles as localized states [5]. And the name "skyrmion" after Skyrme implies these localized solutions.

From the other side, the instability of multidimensional localized states may be avoided in condensed matter systems

*leonov@hiroshima-u.ac.jp
†c.pappas@tudelft.nl
‡ivan.smalyukh@colorado.edu

with broken inversion symmetry, where chiral interactions (energy terms linear with respect to spatial derivatives of order parameters) play a crucial role in their stability. In condensed matter physics chiral interactions arise due to structural handedness. Particularly, in magnetic noncentrosymmetric crystals chiral asymmetry of exchange interactions originates from relativistic Dzyaloshinskii-Moriya coupling [6,7]. Phenomenologically, the Dzyaloshinskii-Moriya interaction (DMI) is expressed as the first derivatives of the magnetization **M** with respect to the spatial coordinates, the so-called Lifshitz invariants (LI)

$$\mathcal{L}_{i,j}^{(k)} = M_i \partial M_j/\partial x_k - M_j \partial M_i/\partial x_k. \quad (1)$$

DMI can stabilize one-dimensional (spirals or helices [8]) and two-dimensional (skyrmions) states with a fixed sense of the magnetization rotation. In particular, solutions for chiral magnetic skyrmions as static states localized in two dimensions were derived first in 1989 [9]. It was shown that these topological solitonic field configurations exist in magnetic systems for all noncentrosymmetric crystallographic classes that allow Lifshitz invariants (1) in their magnetic free energy [9,10].

Chiral interactions having the same functional form as (1) may appear also in many other systems: in ferroelectrics with a noncentrosymmetric parent paraelectric phase, noncentrosymmetric superconductors, multiferroics [11–13], or even in metallic supercooled liquids and glasses [14]. Localized states in these systems are also named skyrmions by analogy with the Skyrme model for mesons and baryons [5].

Chiral liquid crystals (CLC) are considered as ideal model systems for probing behavior of different modulated structures on the mesoscopic scale [15]. In these systems, a surprisingly large diversity of naturally occurring and laser-generated topologically nontrivial solitons with differently knotted nematic fields were recently investigated [15–17]. In particular, the toron represents a localized particle consisting of two Bloch points at finite distance and a convex-shaped skyrmion stretching between them [15,18,19]. In chiral liquid crystals, the acentric shape of underlying molecules is at the heart of chiral effects.

In the last years, there has been a renewed interest in studies of multidimensional topological solitons in chiral magnets and liquid crystals inspired by the discovery of two-dimensional magnetic skyrmions. Due to their nanometer size, topological protection, and the ease with which they can be manipulated by electric currents, the magnetic skyrmions are considered as promising objects for the next-generation memory and logic devices. In particular, in the skyrmion racetrack [20–22]—a prominent model for future information technology — information flow is encoded in isolated skyrmions (IS) [23] moving within a narrow strip. CLC skyrmions with a typical size of several micrometers can also be set in a low-voltage-driven motion with the precise control of both the direction and speed [24]. The CLC skyrmions are confined in a glass cell with thickness comparable with the helicoidal pitch, an CLC counterpart of a race-track memory. The most obvious application of CLC skyrmions, however, is envisioned in various photonic crystal lattices and diffraction gratings, especially if one recalls others textures realized in liquid crystals and based on the different types of defects. In CLCs, these skyrmions are elements of the second homotopy group [25] and contain smooth but topologically nontrivial, spatially localized structures in the alignment field of constituent rod-like molecules, the director field $\mathbf{n}(\mathrm{r})$. They are characterized by integer-valued topological invariants, the skyrmion numbers [25].

In thin layers of cubic helimagnets, skyrmions remain essentially two-dimensional (2D), but gain their stability due to the additional surface twists [26–29] involving the LIs $\mathcal{L}_{x,y}^{(z)}$ with the magnetization derivative along z. These skyrmions were first directly observed in nanolayers of cubic helimagnets $(Fe_{0.5}Co_{0.5})Si$ [30] and FeGe [31] over a broad range of temperatures and magnetic fields. Topologically being elements of the second homotopy group of spheres [32], the two-dimensional magnetic skyrmions can be embedded in thin films or in the bulk of three-dimensional (3D) material systems as translationally invariant structures. However, the 3D configuration/physical space allows for more degrees of freedom in terms of orientation and spatial morphology of axes of these topological solitons, albeit the spectrum of different such possibilities is constrained by energetics of the system.

Bulk magnetic systems represent a truly 3D arena for skyrmion stabilization and manipulation. In particular, bulk helimagnets enable the propagation of skyrmion tubes either along or perpendicular to an applied magnetic field [33,34] and thus may host rather complex topological structures. However, until very recently skyrmions in these systems were found only in a small pocket of their temperature-magnetic field phase diagram, just below the transition temperature T_C, the so-called A phase [35,36]. This restricted their potential as candidates for future spintronic devices. The recent discovery of low-temperature skyrmions in the bulk-insulating cubic helimagnet Cu_2OSeO_3 returned the focus of skyrmionic community to these 3D-embedded skyrmions [37,38]. Moreover, the recent direct visualization of skyrmion clusters with mutually orthogonal orientations in CLC [34] as well as the possibility to construct skyrmionic networks [39] strengthens this motivation. In this sense, skyrmionic superstructures constitute a novel concept of spintronic devices based on gapless skyrmion motion along each other [39].

In the following we will unveil the principles of skyrmion meshing into a large diversity of extended 3D skyrmionic networks and new phases in chiral magnets and liquid crystals. In the next section, we introduce our phenomenological model and the algorithms used for our simulations. Within the continuous and discrete models under consideration, the applied magnetic field is the only control parameter. Thus, we introduce the different critical values of the field to indicate different regimes of the host spiral states that embrace isolated skyrmions. In particular, the field-dependent conical phase may favor a particular type of isolated skyrmions and underlies the strength of the skyrmion coupling and thus the mutual distances between them.

In Sec. III, we examine the internal structure of IS tubes propagating correspondingly along and perpendicular to the wave vector of the conical state. The constructed 3D models provide a straightforward explanation of the attractive nature of skyrmion-skyrmion interaction. In Sec. IV, we consider the winding of a horizontal (H) skyrmion around another vertical (V) one driven by the strong interaction energy between the two. Depending on the cluster configuration, this may lead to a

family of so called target-skyrmions with alternating topological charge ($Q = 0,\ 1$) or to complex multiple-Q target states. We also indicate that the wiggling instability of H-skyrmions may lead to spring-like states that may be seen as a missing intermediate element between H- and V-skyrmions (Sec. V). Finally, we consider the problem of skyrmion stability within the chiral soliton lattice for a field perpendicular to the cone wave vector (Sec. VI). Whenever possible, we discuss connections of our theoretical results to the experimental findings in different condensed-matter systems.

II. PHENOMENOLOGICAL MODEL

In modern skyrmionics, the phenomenological functionals introduced by Dzyaloshinskii in their most basic form, see Eq. (2), are being used as main models for the interpretation of experimental results in different classes of noncentrosymmetric magnetic materials and beyond as a general foundation for the study of modulated phases [40–42] (see bibliography in Refs. [10,43–46] for earlier reviews). It is remarkable that all effects on the 2D and 3D scales can be treated by the same basic model. To make the model more quantitative and directly related to a particular experiment, one usually supplements it with cubic and exchange anisotropies.

This standard model for magnetic states in bulk cubic noncentrosymmetric ferromagnets is based on the energy density functional [8,47]

$$w = A\,(\mathbf{grad}\,\mathbf{m})^2 + D\,\mathbf{m}\cdot\mathrm{rot}\,\mathbf{m} - \mu_0 M\mathbf{m}\cdot\mathbf{H}, \qquad (2)$$

which includes the exchange stiffness and the Dzyaloshinskii-Moriya constants, A and D respectively, as well as the Zeeman energy. These are the principal interactions needed to stabilize all modulated states under scrutiny, e.g., one-dimensional (1D) spiral states and two-dimensional (2D) chiral skyrmions (which may become truly 3D with the structure modulations along the complementary third coordinate). $\mathbf{m} = (\sin\theta\cos\psi; \sin\theta\sin\psi; \cos\theta)$ is the unity vector along the magnetization vector $\mathbf{M} = \mathbf{m}M$. $\mathbf{H}$ is a magnetic field, which will be applied both along z and in the transverse plane.

For the forthcoming calculations, we use nondimensional variables defined in a consistent way with Ref. [10]. The lengths are expressed in units of $L_D = A/D$, i.e., the length-scales are related to the period of the spiral state in zero field $p_0 = 4\pi L_D$, and reflect the fact that the ground state of the system in the form of a single-harmonic mode is yielded as a result of the competition between the counteracting exchange and DM interactions in Eq. (2). Thus L_D introduces a fundamental length characterizing the magnitude of chiral modulations in non-centrosymmetric magnets. $h = H/H_D$, where $H_D = D^2/(AM)$, is the reduced magnitude of the applied magnetic field. To obtain particle-like states within the model Eq. (2), we use finite-difference discretization on rectangular grids with adjustable grid spacings and periodic boundary conditions. The minimization procedure is described in exhaustive detail in Ref. [48].

A. Analitical solutions for cones and helicoids

In the present paper as a host for isolated skyrmions, we consider spiral states with the wave vector $\mathbf{q}$ exclusively along the z axis. For a magnetic field co-aligned with $\mathbf{q}$, a conical spiral retains its single-harmonic character with

$$\psi = \frac{2\pi z}{p_0}, \quad \cos\theta = \frac{2|\mathbf{H}|}{H_D}, \qquad (3)$$

where ψ is the azimuthal angle. In such a helix the magnetization component along the applied field has a fixed value $M_\perp = M\cos\theta = 2MH/H_D$ and the magnetization vector $\mathbf{M}$ rotates within a cone surface. In this case, the conical state combines properties of the homogeneous state and the flat spiral as a compromise between Zeeman and DM energies and represents the global minimum of the functional Eq. (2). The critical value

$$h_c = 0.5 \qquad (4)$$

marks the saturation field of the cone phase into the homogeneous state.

If a magnetic field is directed along the x or y axes, i.e., in the case where the propagation vector $\mathbf{q}$ of a spiral state is perpendicular to an applied magnetic field, the spiral state transforms into a chiral soliton lattice (CSL) [8,49]. While the polar angle retains its constant value $\theta = \pi/2$, the azimuthal angle ψ is expressed as a set of elliptical functions and describes a gradual expansion of the CSL period with increased magnetic field. In a critical magnetic field

$$h_h = \pi^2/8 = 0.30843 \qquad (5)$$

the CSL infinitely expands and transforms into a system of isolated noninteracting 2π-domain walls (kinks) separating domains with the magnetization along the applied field. The CSL is a metastable solution of the functional Eq. (2) since the conical state with $\mathbf{q}$-vector co-aligned with the field is the global minimum. However, it is instructive to consider isolated skyrmions also within this metastable CSL state since the $\mathbf{q}$-vector may be pinned by additional anisotropic contributions and may retain its perpendicular orientation with respect to the field. Such a behavior was recently observed, e.g., in the polar magnetic semiconductor GaV_4S_8. The cycloid states were found to point along the $\langle 110\rangle$ directions irrespective of the field orientation [50]. For a magnetic field perpendicular to the $\mathbf{q}$-vectors, the conical state becomes the global minimum of the system. A magnetic field in the plane of the magnetization rotation, however, leads to a CSL resulting to the reported anomalies of the phase diagrams [51].

Thus, the solutions for cones (3) and helicoids (5) are analytical solutions obtained by minimization of (2) using the Euler equations. Interestingly, at the beginning of skyrmionics, analytical solutions for skyrmions were obtained, as well, as ansatz solutions [9]. For this purpose, no numerical methods were needed, but rather a variational analysis.

B. Energy minimization

For 3D simulations, the Euler-Lagrange equations derived from the energy functional Eq. (2) are nonlinear partial differential equations. These equations were solved by numerical energy minimization procedure using finite-difference discretization on grids with adjustable grid spacings and periodic boundary conditions. Components of the magnetization vector $\mathbf{m}$ were evaluated in the knots of the grid, and for the

calculation of the energy density Eq. (2) we used finite-difference approximation of derivatives with different precision up to eight points as neighbors. To check the stability of the numerical routines we additionally refined and coarsened the grids. For axial fields, we used grid spacings $\Delta_y \approx \Delta_x$ so that grids are approximately square in the xy plane in order to reduce the artificial anisotropy incurred by the discretization. The final equilibrium structure for the 3D particle-like states was obtained according to the following iterative procedure of the energy minimization using simulated annealing and a single-step Monte Carlo dynamics with the Metropolis algorithm as follows.

(i) The initial configuration of magnetization vectors in the grid knots for Monte Carlo annealing was chosen appropriately to ensure relaxation to a desired particle-like state.

(ii) A point (x_n, y_n, z_n) on a grid is chosen randomly. Then, the magnetization vector in that point is rotated without change of its length. If the energy change ΔH_k associated with such a rotation is negative, the new orientation is kept.

(iii) However, if the new state has the energy higher than the last one, it is accepted probabilistically. The probability P depends upon the energy and a kinetic cycle temperature T_k:

$$P = \exp\left[-\frac{\Delta H_k}{k_B T_k}\right], \tag{6}$$

where k_B is Boltzmann constant. Together with probability P a random number $R_k \in [0, 1]$ is generated. If $R_k < P$ the new configuration is accepted otherwise is discarded. Generally speaking, at high temperatures T_k, many states will be accepted, while at low temperatures, the majority of these probabilistic moves will be rejected. Therefore, one has to choose appropriate starting temperature for heating cycles.

(iv) The characteristic spacings Δ_x, Δ_y, and Δ_z are also adjusted to promote the energy relaxation. The procedure is stopped when no further reduction of energy is observed.

III. SKYRMIONS WITHIN THE CONICAL STATE

In this section we consider the internal structure and characteristic features of skyrmions within the conical state for $\mathbf{h}||z$. In cubic helimagnets ISs may orient themselves either along or perpendicular to the field.

The internal spin pattern of V-IS with their axes along the wave vector of the conical phase is depicted in Figs. 1(a) and 1(b). In the field range $[0, h_c]$, the magnetization distribution in a cross-section xy splits into the central core region that nearly preserves the axial symmetry [Fig. 1(a)] and the domain-wall region, connecting the core with the embedding conical state. This part of the skyrmion cross-section is *asymmetric* and acquires a crescent-like shape, which undergoes additional screw-like modulation along z axis, matching the rotating magnetization of the conical phase [Fig. 1(b)].

A convenient way to depict these skyrmions, which has been proven to be particularly illustrative in addressing the character of skyrmion-skyrmion interaction, is as follows [Fig. 1(c)]: we extract the spins corresponding to the conical phase and then plot the remaining spins as spheres colored according to their m_z-component. In this way, all intricate details of the internal structure are explicitly revealed, which spares the difficulties to plot skyrmion crosscuts along the different directions. In such a fashion, V-skyrmions are composed of a cylinder-like (blue) core centered around the magnetization opposite to the field and a (red) coil with the magnetization along the field [Fig. 1(c)]. Current experimental endeavors are particularly focused on unveiling the three-dimensional spin texture of skyrmion tubes [28,29,52–54].

The cluster formation of V-skyrmions may be envisioned as a process of zipping loops: a coil of one V-skyrmion penetrates the voids between the coils of another one [Fig. 1(d)]. By this, the compact skyrmion pair recreates a fragment of a SkL that within the model Eq. (2) is a metastable state: the magnetization on the way from the center of one skyrmion to the center of another rotates as in ordinary axisymmetric skyrmions.

The attraction of V-IS mediated by the conical phase was considered theoretically in Refs. [24,55–58]. Experimentally, clusters of such skyrmions have been observed in thin (70 nm) single-crystal samples of Cu_2OSeO_3 taken using transmission electron microscopy [59] and in nematic fluids, where they were shown to also form skyrmion chains [24]. In the following, we refer to the experiments on both the chiral magnets and chiral liquid crystals that support these theoretical results.

For $h > h_c$ with the onset of the homogeneous state, V-ISs loose their coils and acquire an axisymmetric structure localized in nanoscale cylindrical regions [Fig. 1(e)] thus representing ensembles of weakly repulsive particles. The repulsion of conventional axisymmetric V-skyrmions within the saturated state was investigated in Ref. [60] and it was shown that the region where V-skyrmions persist at high fields is defined by their collapse. The field-driven evolution of V-skyrmions is driven by their decreasing energy from the most distorted state within the conical phase at $h = 0$ to the axially symmetric particles at higher fields [red curve in Fig. 1(f)].

Horizontal skyrmions perfectly blend into the spiral state and for $h = 0$ they represent a pair of merons with equally distributed topological charge $Q = 1/2$. Figures 1(h) and 1(i) show the evolution of such a meron pair into a distorted isolated skyrmion. Red and blue areas in Figs. 1(h) and 1(i) correspond to positive and negative values of the m_y-component. Following the same paradigm of excluded cone spins, H-skyrmions are displayed in Fig. 1(j) as two parallel distorted cylinders centered around the core (blue) and the transitional region (red) with the negative and the positive m_z component of the magnetization, correspondingly. For consistency, we run H-skyrmions along the y axis and keep in mind that these may exist with positive and negative polarities, i.e., directions of the magnetization in the region between two cylinders.

The evolution of H-skyrmions with increasing magnetic-field is shown in Fig. 1(j). At higher fields, they have nonaxisymmetric structures on the xz plane and within a given accuracy of the excluding spin procedure, the "red" counterpart of H-skyrmions disappears altogether within the ferromagnetic surrounding. Thus, the field-driven transformation of H-skyrmions leads to a clear energetic disadvantage at higher fields [blue curve in Fig. 1(f)]. Once embedded into the conical phase, H-skyrmions develop an attracting interaction, which becomes repulsive within the homogeneous state. According to the authors Refs. [39,61], two coupled

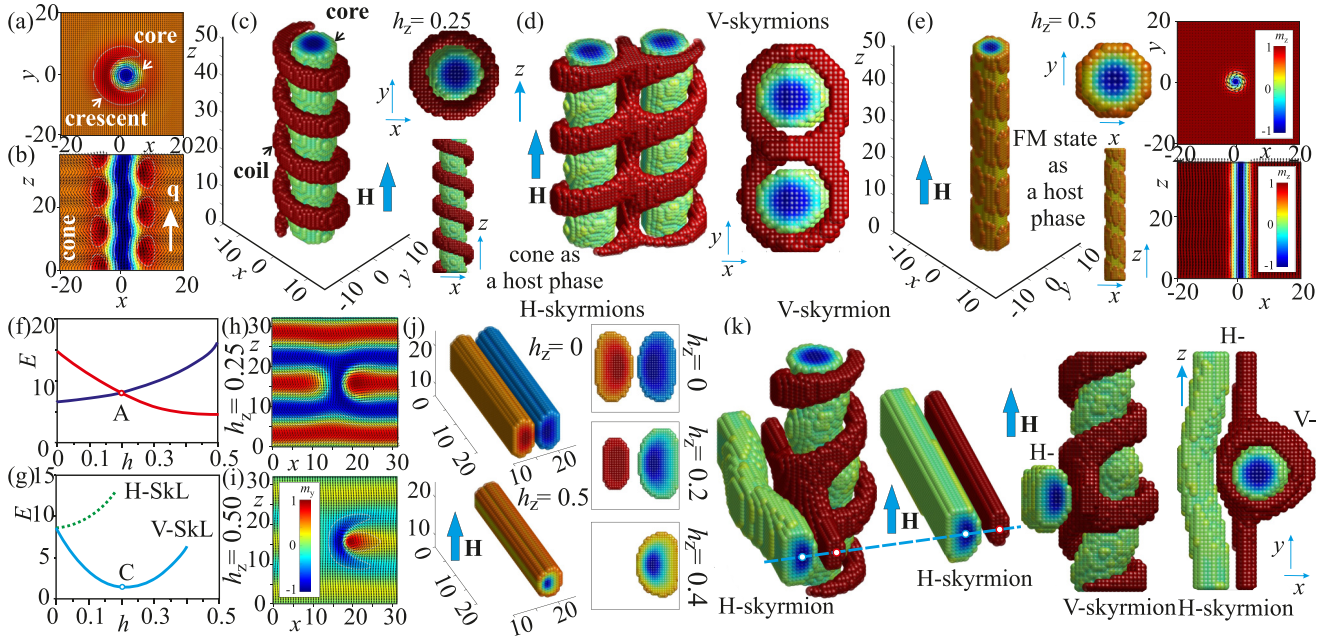

FIG. 1. (a)–(e) Magnetic structure of vertical skyrmions showing their evolution from the nonaxisymmetric structure within the conical phase for $h = 0.25$ (a)–(c) to the axisymmetric structure for (e) $h = 0.5$. In (a) the structure of an isolated skyrmion is represented as a color plot of m_z component of the magnetization with arrows indicating projections of the magnetization onto the xy plane. Since the twisting magnetization **m** in the vertical skyrmions matches boundary conditions imposed by the surrounding conical phase, the internal structure represents notably an axisymmetric core surrounded by a crescent-shaped transitional region [marked by white lines in (a)]. In (b), the internal structure of a vertical skyrmion is shown in the xz cross-section. In (c) and (e) we use an alternative way of representing the internal structure of vertical skyrmions. After we extracted the magnetization components corresponding to the conical phase, the vertical skyrmion represents a cylinder-like core centered around the magnetization opposite to the field and a coil with the magnetization along the field [the corresponding regions are also marked by arrows in (c)]. Subsets in (c) and (e) show projections of such 3D constructs onto the xy and xz planes. Then, the cluster formed out of two vertical nonaxisymmetric ISs in (d) recreates the fragment of a metastable skyrmion lattice with the homogeneous state between two skyrmions. Such a homogeneous state is formed if the coils of two skyrmions are getting "zipped" together. Axisymmetric skyrmions in (e), on the contrary, develop a repulsive interaction as can be judged from their internal structure. Internal structure of horizontal skyrmions is shown in the same way as color plots of the magnetization within the conical phase for (h) $h = 0.25$ and within the homogeneous state for (i) $h = 0.5$. Note that the color plots in this case reflect the m_y component of the magnetization. m_x and m_z components of the magnetization are shown by black arrows. By using the 3D constructs with excluded spins of the conical phase, the horizontal skyrmions represent tubes running for definiteness along y axis (j). Subsets in (j) exhibit projections of such tubes onto the plane yz and demonstrate that with the increasing magnetic field a horizontal skyrmion represents just one tube with the magnetization opposite to the field. Interaction between horizontal and vertical skyrmions is shown in (k). The transient red region of one H-skyrmion may either slide in-between the coils of a V-skyrmion or just touch its coil if located on the other side. Thus, one may distinguish two energetically different cluster configurations. Energies of V- and H-skyrmions above the host conical state (red and blue curves, correspondingly) in (f) indicate the metastability of considered skyrmions since their energies are positive. At the same time, (f) exhibits the crossover between two types of isolated skyrmions [point A in (f)]. This means that the region of cluster formation embraces an intermediate field range below the cone saturation h_c. Energy densities of skyrmion lattices composed from the skyrmions of just one type are shown by solid blue and dashed green lines in (g) and indicate cogent preference of V-SkLs (see text for details).

H-skyrmions are energetically more favorable than two distant ones. However, the energy difference between these two configurations is almost negligible. Therefore, these clusters are less coupled than the corresponding clusters of V-skyrmions, which have a much higher dissociation energy, up to 30%, in comparison to the energy of V-ISs [55].

A consequence of the above-mentioned considerations is that the crossover between the two types of ISs (dubbed a skyrmion flop transition in Ref. [39] or toggle-switch-like crossover in Ref. [33]) takes place for an intermediate value of the field $h \approx 0.2$ [Fig. 1(f)]. Furthermore, there is an obvious advantage of V-skyrmion clustering to SkLs composed of skyrmions of the same type [Fig. 1(g)].

Cluster formation of mutually orthogonal skyrmion tubes [Fig. 1(k)] is also possible, as shown in Ref. [34]. The energy gain due to the clustering of H- and V-skyrmions was shown to reach the same high value of 30% in comparison to the energy of uncoupled ISs. For coupled H- and V-skyrmions one may distinguish two cluster configurations [Fig. 1(k)]. Indeed, the transient red region of one H-skyrmion may either slide in-between the coils of the V-skyrmion or just touch its coil if located on the other side. Here we notice, however, that within the basic model Eq. (2) both skyrmion varieties have a positive energy with respect to the host phase.

Both regimes of skyrmion interaction were directly visualized in the chiral nematic mixtures [34]. In these experiments,

the V- and H-skyrmions were controllably "drawn" into the CLC cells using optical tweezers. Additionally, they were manipulated by the focused laser beams and spatially translated within the sample plane. Because of the CLCs preference to twist, the skyrmions were proved to be topologically stable excitations in the conical background.

In chiral cubic helimagnets magnets, however, clusters of mutually orthogonal skyrmions may account for the anomalies within the A-phases provided the ISs have a negative energy with respect to the surrounding conical state. This would underlie the nucleation processes of skyrmion filaments via torons [18,19]. In these systems the problem of V-skyrmion stability is fully resolved in contrast to that of H-skyrmion stability, which is still unknown. Indeed, the stabilization/nucleation mechanism of V-skyrmions is based on the deformations, imposed by small anisotropic contributions, to their main competitor—the conical phase—rather than on themselves. In particular, uniaxial anisotropy of the easy-axis type [62], which does not affect the ideal single-harmonic type of the magnetization rotation in the conical spiral but just leads to the gradual closing of the cone, grants the thermodynamical stability of the V-SkL in a broad region of theoretical and experimental phase diagrams [63–65]. Cubic anisotropy also stabilizes V-SkLs but for specific directions of the applied magnetic field [38,66–68]. This anisotropy deforms the ideal conical configuration as the magnetization tends to deviate from the ideal conical surface trying to embrace the easy axes and to avoid the hard directions.

In the case of H-skyrmions, however, any manipulation of the conical phase does not necessarily improve the skyrmion's stability. On the contrary, it may even increase the eigenenergy of H-skyrmions.

In case there is a stabilization mechanism suitable for both skyrmion species, H-skyrmions will lower their energy around the most undistorted state at $h_z = 0$ whereas V-skyrmions will be stabilized at rather high fields, These two species would thus be responsible correspondingly for zero-field and A-phase precursor effects in cubic helimagnets [69,70]. In the following, we do not address the question of skyrmion stability but concentrate on already existing/created metastable H- and V-skyrmions as was done, e.g., in the experiments on chiral nematics [34].

IV. TARGET-SKYRMIONS AS A RESULT OF SKYRMION ADDITION AND/OR SUBTRACTION

Here we consider the attraction between mutually orthogonal skyrmions, which opens up a route for skyrmion addition and/or subtraction. We first treat the case of an H-skyrmion that runs parallel to the y axis in Fig. 1(k) and is ziplocked with a V-skyrmion. Guided by the large negative interaction energy, the H-skyrmion may start to wind around the V-skyrmion penetrating the space between the coils and circling along z. This process leads to further energy reduction with respect to the configuration shown in Fig. 1(k). The obtained target-skyrmion bears a total topological charge of $Q = 0$ and is therefore the result of a topological charge subtraction between the H- and a V-skyrmions. Alternatively, such a composite object can be regarded as a V-skyrmion with $Q = 0$, in which an H-skyrmion contributed to its structure. Here we use the conventional definition of a topological charge

$$Q = \frac{1}{4\pi} \iint d^2 r \mathbf{m} \frac{\partial \mathbf{m}}{\partial x} \frac{\partial \mathbf{m}}{\partial y}. \tag{7}$$

The skyrmion number is a topological invariant describing how many times $\mathbf{m}(r)$ within the single skyrmion wraps around the sphere S_2. For V-skyrmions it remains equal to unity, indicating topological stability with respect to smooth $\mathbf{m}(r)$ deformations prompted by changing magnetic field.

In the transverse plane xy, such a target-skyrmion consists of a doubly twisted core surrounded by a number of concentric helicoidal undulations [Figs. 2(a)–2(d)]. Depending on the number of these concentric helical stripes, the topological charge alternates and has the value either 0 (odd number of helical undulations) or 1 (even number). Such target-skyrmions have been recently theoretically predicted [71] and subsequently experimentally observed in magnetic nanodiscs/nanowires [72–74]. They may be energetically favored by both the magnetostatic energy demanding a flux-closed states and by the so-called edge states that supply targets with additional negative energy.

Surprisingly, a target-skyrmion with the topological charge $Q = 2$ is also achievable if an H-skyrmion has its blue part touching the red coil of a V-skyrmion [Fig. 1(k)]. In this case the H-skyrmion will circle around the V-skyrmion, along the z axis, and the two topological charges will be added to the total charge of a target-skyrmion rather than subtract from each other. The composite structure of such a state is illustrated in Figs. 2(e)–2(h). The $(Q = 2)$-target is separated by some potential barrier from the $(Q = 1)$-V-skyrmion since a part of the structure [encircled by a white dashed line in Fig. 2(h)] may annihilate.

Skyrmions with $Q = 2$ are usually obtained via the in-plane magnetization rotation [75,76]: in such skyrmions, the polar angle varies from π to 0, but the azimuthal angle becomes $\psi = Q\varphi + \gamma$. This in general leads to multiple-Q skyrmions [77], which are fundamentally different from the ones considered in Fig. 2(e). Another approach of obtaining high-charge skyrmions involves construction of so-called "skyrmion bags" [25], which are translationally invariant along the skyrmion bag's tube and also fundamentally different from the ones considered in Fig. 2(e), even if they can also be realized in chiral magnets and liquid crystals.

In general, by winding H-skyrmions around V-skyrmions one may achieve a family of target-skyrmions with either $Q = 0$ or $Q = 1$, depending on the energetically stable cluster configuration. Thus, to create a target-skyrmion with $Q = 1$ out of that in Fig. 2(a), one should slide an H-skyrmion with its blue part between the blue coils of a current target-skyrmion. On the other hand, to create a target-skyrmion with $Q = 3$ out of that in Fig. 2(e), the blue part of an H-skyrmion should touch a red coil of a current target-skyrmion.

V. SKYRMION SPRINGS WITH POSITIVE AND NEGATIVE POLARITIES

The wiggle instability of H-skyrmions may also be guided by the much smaller interaction energy that underlies the attraction between them [39,61]. Also provided that H-ISs acquire negative energy, their bending would serve the

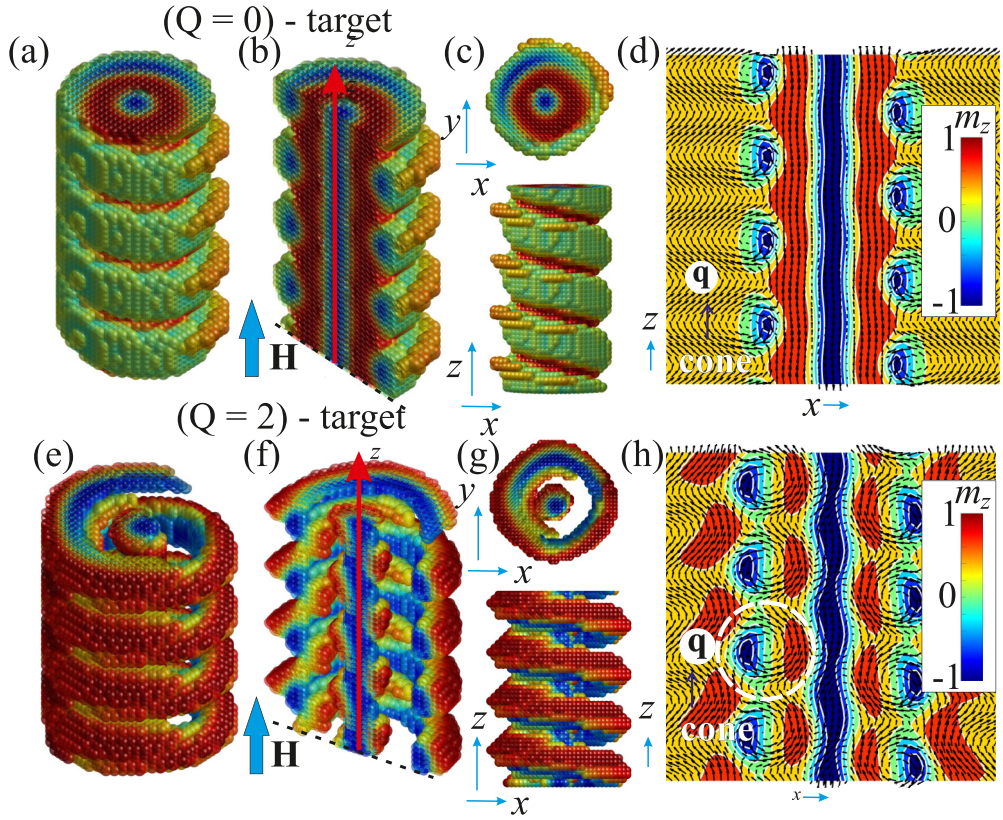

FIG. 2. Internal structure of target skyrmions with either an alternating topological charge [(a)–(d) $Q = 0; 1$] or the multiple Q [(e)–(h) $Q = 2$]. In (a)–(c) and (e)–(g) we plot the internal structure of target-states in the following way: we extract the spins corresponding to the conical phase and then plot the remaining spins as spheres colored according to their m_z-components. Then, such 3D constructs for two types of target-states are shown in (a) and (e). To reflect the core structure of target skyrmions, we also plot their halves intersected by the xz plane as depicted in (b) and (f). Here, the red arrow represents the z axis, the blue arrow indicates direction of the applied magnetic field. In (c) and (g), we plot projections of the corresponding 3D constructs onto the xy and xz planes. Target skyrmions originate as a result of swirling of H-skyrmions around a V-skyrmion by the tendency to reduce the interaction energy. Thus, two energetically different situations can be distinguished. In the first one, one winds consecutively horizontal skyrmions around one vertical skyrmion and always achieves an energetically favorable structure according to the skyrmion-skyrmion interaction depicted in Fig. 1(k) (see a horizontal skyrmion to the left). (a)–(d) Then, one will get a family of targets with the alternating topological charge 0 or 1. If, on the contrary, one winds a horizontal skyrmion around a vertical one according to the energetically unfavorable situation like in Fig. 1(k) (see a horizontal skyrmion to the right), then each successive horizontal skyrmion will add its topological charge and results in a target state depicted in (e)–(h). In (d) and (h), the structure of target skyrmions is represented as color plots of m_z-component of the magnetization with arrows indicating projections of the magnetization onto the xz plane. The wave vector of the conical spiral $\mathbf{q}$ points to z axis. By the dashed white circle in (h) we show the part of the magnetization distribution that can annihilate and thus lead to an ordinary V-skyrmion with the topological charge $Q = 1$. Legends show the color scheme for m_z component: red color stands for $m_z = 1$, and blue for $m_z = -1$.

tendency to occupy the entire space, thus being an alternative mechanism to skyrmion condensation into a skyrmion lattice.

However, if H-skyrmions bend, they change their altitude along z. Indeed, in Fig. 3(a) two straight H-skyrmions running along x and y axes (marked by numbers #1 and #2) differ by the value πL_D of their relative z coordinate. Another $\pi/2$-rotation results in an H-skyrmion running opposite to y axis (marked by #3) and thus having an opposite polarity to that along the y axis. The full rotation by 2π leads to two skyrmions stacked above each other at the distance p. The sense of H-skyrmion circling is fully defined by the encompassing conical phase (counterclockwise in the present case) and is therefore unique.

Wiggling of H-skyrmions may also give rise to exotic textures in the form of skyrmionic springs, which exist in two varieties with the positive (red) and/or the negative (blue) part facing the interior [Figs. 3(c)–3(f)]. Since within the basic model Eq. (2) such springs possess positive energy over the conical phase, they gradually shrink and in this way transform into corresponding V-skyrmions with a positive or negative topological charge depending on their polarity [Figs. 3(d) and 3(f)]. In this sense, such springs can be considered as an intermediate link between two skyrmion varieties. In general, springs with variable radius could also be envisioned, but in this case the interaction energy is not fully minimized since the overlap region of H-skyrmions diminishes. We also notice that even one loop of a spring contracted to a patch of a V-skyrmion (which then represents a toron [18,19]) provides a new mechanism of skyrmion nucleation, i.e., looping H-skyrmions gives rise to torons, which subsequently may be instigated to stretch along the z axis owing to, e.g., cubic anisotropy.

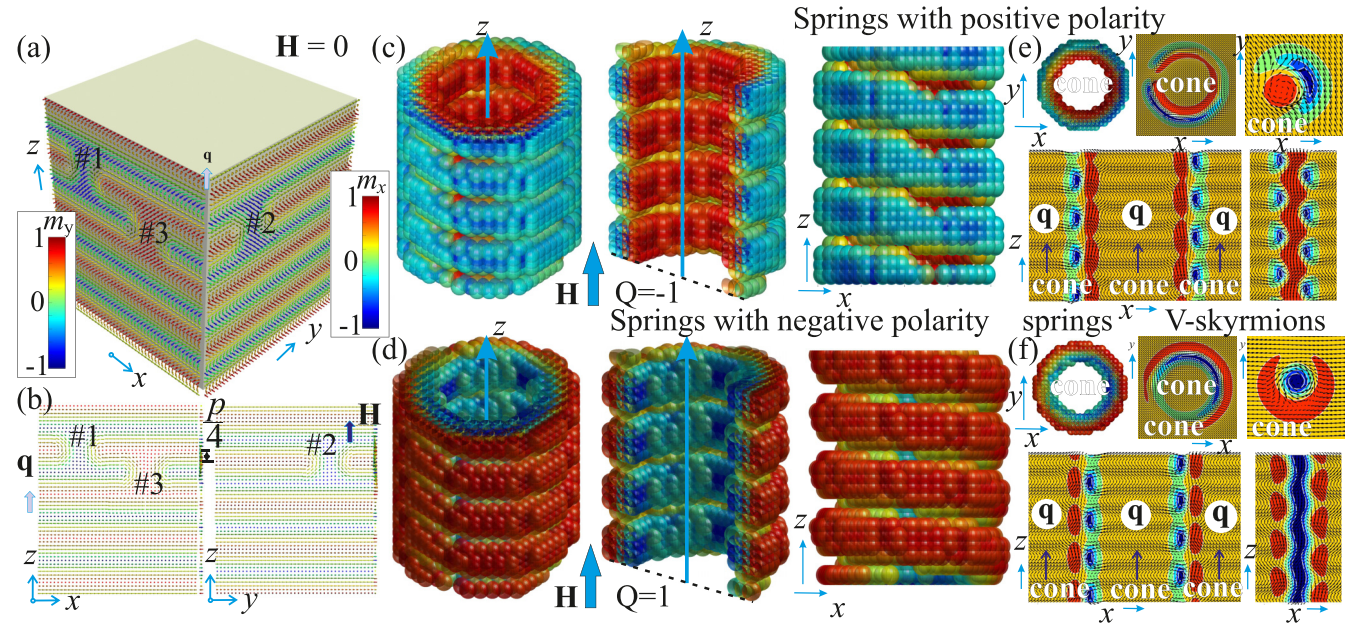

FIG. 3. Internal structure of spring-like states obtained by swirling of H-skyrmions around z axis and guided by the small interaction energy. First of all we notice, (a) if H-skyrmions bend, they change their altitude along z. Two straight H-skyrmions running along x and y axes in (a) (marked by numbers 1 and 2) differ by the value $p/4$ of their relative z coordinate. Another $\pi/2$-rotation results in an H-skyrmion running opposite to y axis (marked by 3) in (a) and thus having an opposite polarity to that along the y axis. Thus, the full rotation by 2π leads to two skyrmions stacked above each other at the distance of the spiral period p. (b) shows corresponding facets of the cube in (a). Legends show the color scheme for m_y component: red color stands for $m_y = 1$, and blue for $m_y = -1$. In (c) and (d) we plot the internal structure of spring-like states in the following way: we extract the spins corresponding to the conical phase and then plot the remaining spins as spheres colored according to their m_z-components. Then, such 3D constructs for two types of spring-states are shown in (c) and (d). To reflect the core structure of spring states, we also plot their halves intersected by the xz plane as depicted in the second panels of (c) and (d). Here, the blue thin arrow represent the z axis, the blue thick arrow indicates direction of the applied magnetic field. In the third panel of (c) and (d), we plot projections of the corresponding 3D constructs onto the xz planes. Depending on the interior, the springs acquire either the (c) positive or (d) the negative polarity, as well as the negative and the positive topological charges. In (e) and (f), the structure of spring-states is represented as color plots of m_z-component of the magnetization with arrows indicating projections of the magnetization onto the xz plane [lower panel of (e) and (f)] and xy plane (upper panels). The wave vector of the conical spiral $\mathbf{q}$ points to the z axis. Being metastable particle-like states, the spring-like states gradually shrink and in this way transform into V-skyrmions what is shown by the corresponding color plots in (e) and (f).

The considered 3D springs with a constant tube radius along z can be considered as relatives of 2D Archimede's spirals. In CLC, these spirals are produced by the transverse drift of fingers of the second type [78]. Since the fingers are confined within the thin film by the surface anchoring, their wiggling instability results in spiraling with the same altitude along z and thus leads to a number of spiral turns.

Beyond CLCs, such Archimede's spirals may exist in garnet ferrite films [79,80], where they are surrounded either by the labyrinth domain structure or by the bubble magnetic domains and are stabilized by the dipole-dipole interactions. By turn, the bending of stripe domains in garnet-ferrites reflects the geometry of easy anisotropy axes or their projections onto the basal plane. The structure of Archimedes's spirals was also addressed numerically in chiral helimagnets within two host phases—spirals and SkL [81]. Thus in some sense, the considered 3D springs (Fig. 3) may be regarded as Archimedes's spirals escaping into the third dimension, but also driven by the mutual attraction between adjacent loops. Interestingly, geometrically more complex structures with local fragments resembling H-skyrmions can yield a hopfion of the so-called "heliknoton" type, a topological solitons described by the third homotopy group elements as topological invariants [82].

VI. ISOLATED SKYRMIONS WITHIN THE METASTABLE SPIRAL STATES FOR AN IN-PLANE MAGNETIC FIELD

In the following, we examine the structure of H- and V-skyrmions within the spiral state $\mathbf{q}||z$ for an in-plane direction of the field $\mathbf{H} \perp z$. In this case, the complex 3D internal structure of magnetic ISs and the character of the IS-IS interaction are imposed by a surrounding parental state as investigated in detail in Refs. [34,39]. On the other hand, however, ISs themselves distort the structure of their host and in this way they influence its field-driven evolution.

V-skyrmions, which retain their positive energy even over a metastable spiral state [Fig. 4(a)], are found also to impede a gradual expansion of the helicoid period with the critical field h_h Eq. (5) [Fig. 4(b)]. For low values of the field, V-skyrmions stimulate spirals to slightly expand to release their own structural distortions, which lead to a high positive energy.

In Fig. 1(f), the energy of a V-skyrmion in zero field was computed with the fixed period $p = 4\pi L_D$ of a spiral state. However, some energy reduction can be achieved for a larger spiral period [Fig. 4(b)]. With an increasing magnetic field, however, a V-IS defers the spiral expansion since this process would lead to the increase of its own energy. As a result, the

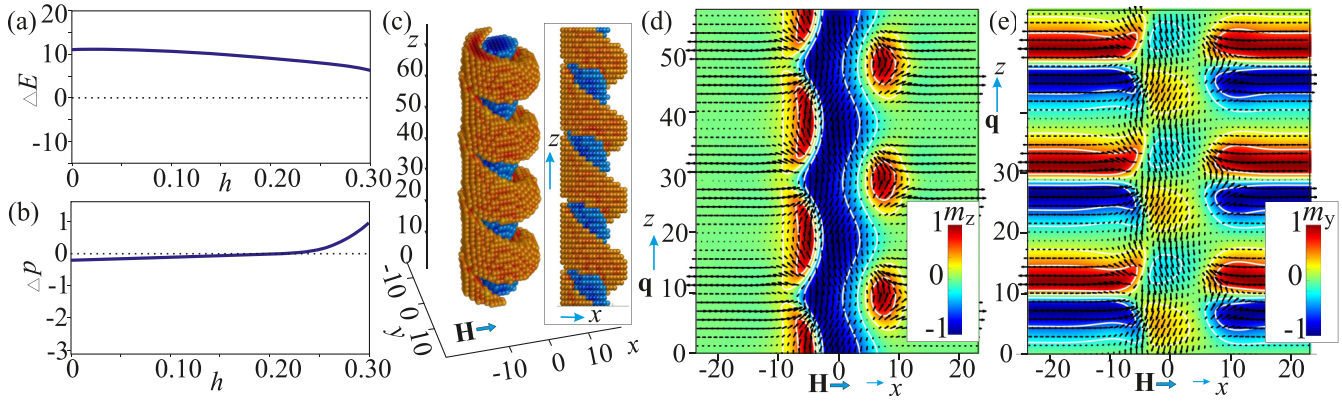

FIG. 4. Field-driven deformation of a V-skyrmion within the chiral soliton lattice for the in-plane direction of the magnetic field, $\mathbf{H} \perp z$ (see text for details). Color plots exhibit (d) m_z and (e) m_y components of the magnetization with the arrows showing projection of the magnetization onto the xz plane. Alongside with the (c) 3D skyrmion model, the pictures demonstrate broadening of skyrmion loops along the field and narrowing otherwise, which is consistent with the spiral behavior in the field perpendicular to its wave vector. The eigenenergy of a V-skyrmion remains positive with respect to (a) the surrounding spiral phase. Still, an isolated skyrmion intervenes into a field dependence of a spiral period (b). At a low magnetic field, a V-skyrmion slightly expands the spiral, whereas for the field near the saturation (5), it slows down a process of spiral expansion. Here Δp is the difference between the periods of spiral states without and with a V-skyrmion.

energy of an IS within the spiral state with a nonequilibrium period, could be reduced. Thus, the internal structure of V-skyrmions shown in Figs. 4(c)–4(e) is balanced by the spiral tendency to acquire an equilibrium period for a given value of the field and the skyrmions' tendency to reduce their length. The skyrmion coils are deformed according to expanding and shrinking parts of a spiral state aligned, correspondingly, along and opposite to the field.

Obviously, the structure of V-skyrmions does not depend on the direction of the field within the plane xy. For H-skyrmions, however, the two cases with $\mathbf{H}||x$ and $\mathbf{H}||y$ should be treated separately. First of all, the H_y-magnetic field lifts the energetic degeneracy of H-skyrmions with the positive and the negative polarities [Fig. 5(a) and 5(b)]. Indeed, the cuts of an expanding spiral state in the form of two merons may occur either in the "wide" or in the "narrow" part of a spiral period[Figs. 5(c)–5(f)] with the latter being energetically more favorable [Fig. 5(a)]. Moreover, the energy of this meron pair becomes negative with respect to the helical background at a critical field $h_y \approx 0.16$ that then gives start to the conventional helicoid-SkL first-order phase transition observed experimentally in thin-film helimagnets [30,31]. The hexagonal arrangement of meron pairs [Fig. 5(h)] is more favorable as compared with the square one [Fig. 5(g)]. Furthermore, a configuration with closely packed skyrmions and merons [Fig. 5(j)] due to a mutual attraction is more favorable than any configuration with dispersed merons [Fig. 5(i)]. Eventually, such a process of meron formation [61,83] and

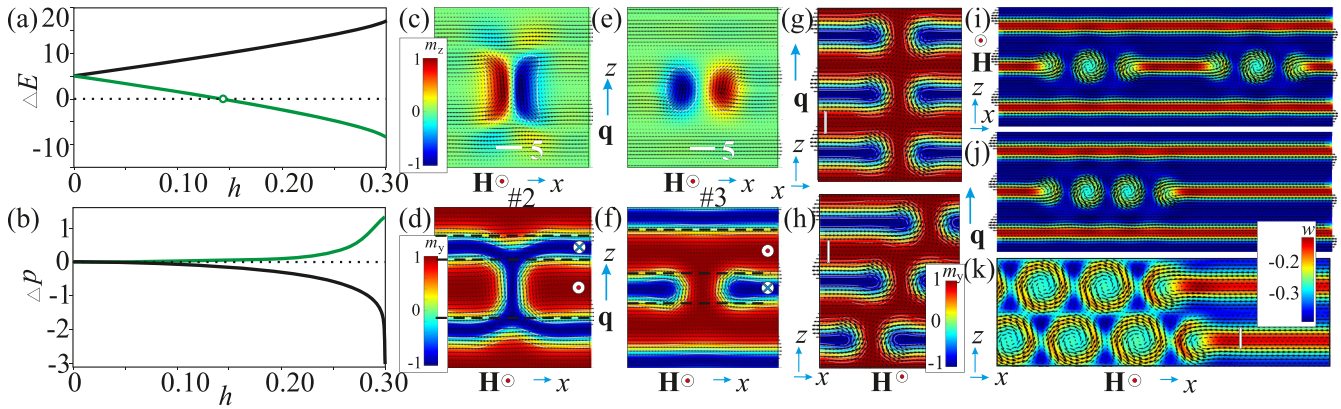

FIG. 5. Field-driven evolution of H-skyrmions for the field coaligned with their axes. Both types of H-skyrmions are exhibited either as color plots of (c), (e) m_z magnetization components or (d), (f) m_y ones and represent cuts of a spiral state in the form of two merons. Whereas a pair of merons with the negative polarity becomes favorite within the spiral state, (a) merons with the positive polarity maintain their positive energy. In the first state, (k) an avalanche-like formation of merons eventually results in a hexagonal skyrmion lattice. The color plot in (k) exhibits an energy density w (2) within the SkL-domain (to the left) and within the spiral domain (to the right). Black arrows indicate corresponding projections of the magnetization onto the xz plane. First of all, (h) a hexagonal-like arrangement of merons is energetically more favorable as compared with (g) the square-like arrangement; then, (j) configurations with the skyrmions gathered together are preferred over (i) their dispersed arrangements. Panel (b) provides information on the distortions of the equilibrium spiral period made by both types of H-skyrmions.

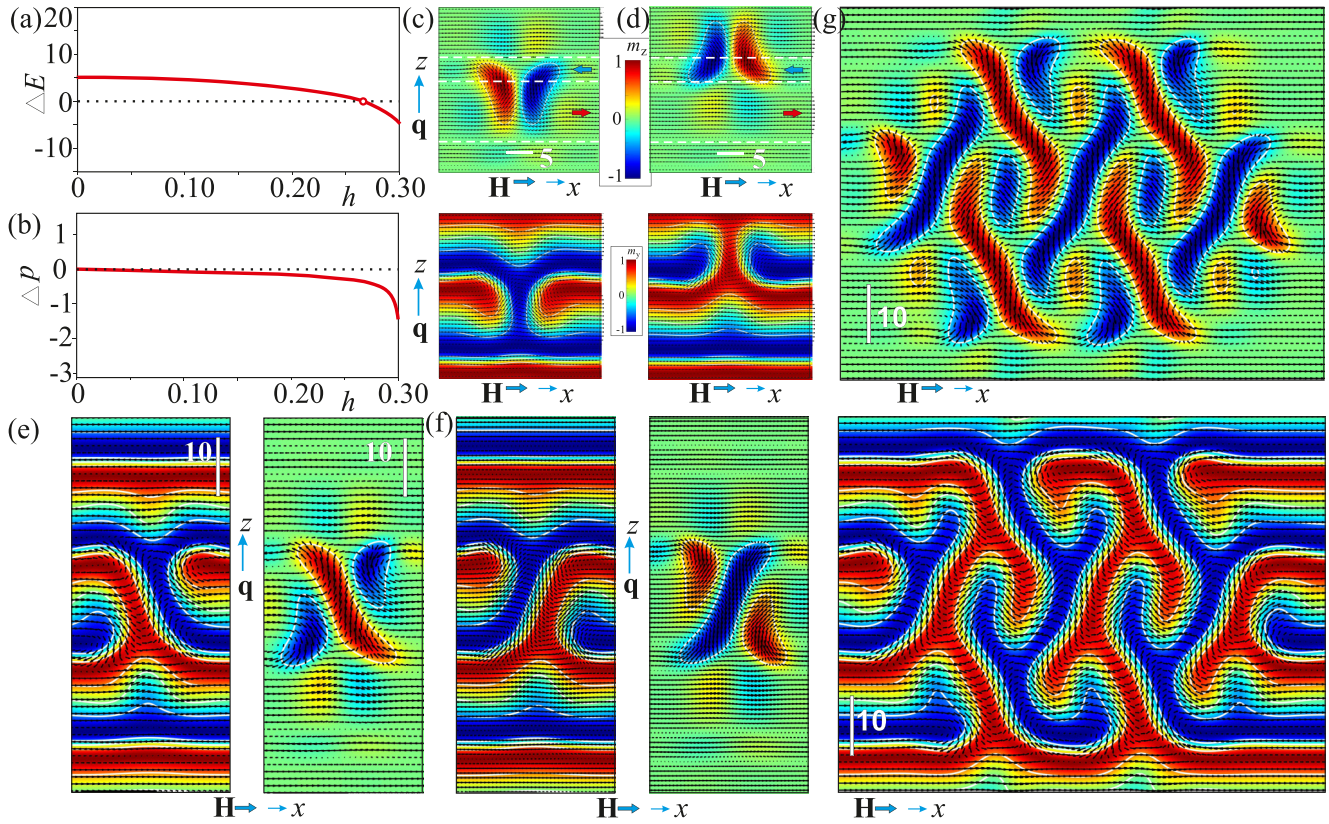

FIG. 6. Field-driven evolution of H-skyrmions for the field perpendicular to their axes. Irrespective of their polarity, H-skyrmions bear the same energy over the host CSL state [red curve in (a)]. (c), (d) The structure of H-skyrmions is shown by the color plots of m_z and m_y components of the magnetization. (g) The first graphical representation appears to be more instructive in elucidating the principles of meshing the H-skyrmions into entangled patterns. First of all, we notice that the energy of H-skyrmions becomes negative in the vicinity of (a) h_h which favors spiral cuts. Then, the (e), (f) structural cross-like elements, obtained as intersections of two H-skyrmions with opposite polarities, may become compositional units of skyrmions superstructures. One of the examples that mixes "crosses" in an involved way is shown in (g) and has smaller energy as compared with the host spiral state. Panel (b) provides information on Δp.

condensation culminates in the hexagonal arrangement of closely packed skyrmions within the skyrmion lattice phase [Fig. 5(k)]. Interestingly, the critical field of the SkL-helicoid phase transition equals $H \approx 0.1H_D$ if based only on the direct comparison of corresponding energies of a helicoid and a hexagonal SkL [10,62], thus, showing a field gap for merons to become energetically advantageous and to initiate an "avalanche"-like phase transition. Since the period of a CSL diverges at the critical field h_h, whereas the period of the SkL—at $h_{sk} \approx 0.4H_D$, a pair of merons [green curve in Fig. 5(b)] slows down a process of a spiral expansion (see Ref. [62] to compare equilibrium periods of spiral and SkL states within the model Eq. (2)). H-skyrmions with the opposite polarity [Figs. 5(c) and 5(d)] remain metastable states in the whole field range with the monotonous energy increase. Such skyrmions thus stimulate the CSL expansion [Fig. 5(b)].

In an H_x-magnetic field, however, the degeneracy of H-skyrmions persists as the two skyrmion configurations with differently oblique positive and negative parts [Figs. 6(c) and 6(d)] bear the same energy [Fig. 6(a)]. Surprisingly, the energy of H-skyrmions becomes negative near the critical field h_h what may result in the same process of meron formation as described previously for $\mathbf{H}||x$. However, besides the obvious square-like or hexagonal-like arrangement of merons, one may consider the emergence of more entangled spin structures. As a basis for these configurations, we consider cross-like states obtained by the intersection of two H-skyrmions with opposite polarities and having positive or negative diagonals as their main elements [Figs. 6(e) and 6(f)]. An example of the periodic dendritic patterns obtained by meshing these cross-like elements is shown in Fig. 6(g) and has negative energy as compared with the host spiral state.

VII. CONCLUSION

To conclude, we introduce an approach for numerical analysis of 3D chiral skyrmions. By scanning the intricate structure of skyrmions and excluding the spins corresponding to the host conical phase, we obtain representative 3D models of horizontal and vertical skyrmions that not only unambiguously characterize the topology of these 3D particles, but also provide tools to envision the process of complex cluster formation.

All our calculations were based on the phenomenological Dzyaloshinskii theory for chiral magnets. Remarkably, this basic model is able to address a range of phenomena rooted in the chiral DMI and is widely used for interpretation of experimental results in noncentrosymmetric magnetic

materials, and beyond as a general foundation for the study of modulated phases and localized states. Moreover, due to the deep connection of phenomenological models for different condensed-matter systems, the results of numerical simulations were shown to successfully address solitonic textures in other condensed-matter systems, in particular, in chiral liquid crystals.

Our work also unravels a path that allows to transform horizontal skyrmions into vertical ones with appropriate polarity, which is achieved via the wiggling instability of H-skyrmions. We speculate that undulations of H-skyrmions may generate torons—nuclei of V-skyrmions that are able to elongate in presence of stabilizing anisotropic interactions. So-called spring-like states appear as ultimate states of such H-skyrmions swirling along the z axis driven by attraction between adjacent loops. A vertical skyrmion, lassoed by a horizontal one, also predefines a direction of their propagation and may lead to a family of target-skyrmions including those with a multiple topological charge.

Finally, we illustrate a reverse impact of isolated skyrmions on the structure of the host spiral states for the field perpendicular to the spiral wave vector. Having a positive energy over the host state, skyrmions affect the process of a field-induced spiral expansion. Acquiring a negative energy, skyrmions initiate a first-order phase transition into a corresponding skyrmion arrangement, which is not necessarily a hexagonal skyrmion lattice: exotic skyrmionic networks can also be envisioned.

ACKNOWLEDGMENTS

The authors are grateful to Ulrich Rößler for useful discussions. A.O.L. thanks Ulrike Nitzsche for technical assistance and acknowledges JSPS Grant-in-Aid (C) 21K03406. C.P. acknowledges financial support from the Vrije FOM program Skyrmionics. I.I.S. acknowledges support of the US National Science Foundation Grant No. DMR-1810513.

[1] A. Schmeller, J. P. Eisenstein, L. N. Pfeiffer, and K. W. West, Evidence for Skyrmions and Single Spin Flips in the Integer Quantized Hall Effect, Phys. Rev. Lett. **75**, 4290 (1995); C. Bäuerle, Yu. M. Bunkov, S. N. Fisher, H. Godfrin, and G. R. Pickett, Laboratory simulation of cosmic string formation in the early Universe using superfluid ^{3}He, Nature (London) **382**, 332 (1996).

[2] U. K. Rößler, A. N. Bogdanov, and C. Pfleiderer, Spontaneous skyrmion ground states in magnetic metals, Nature (London) **442**, 797 (2006).

[3] C. Rebbi and G. Soliani, *Solitons and Particles* (World Scientific, Singapore, 1984).

[4] R. H. Hobart, On the instability of a class of unitary field models, Proc. Phys. Soc. Lond. **82**, 201 (1963); G. H. Derrick, Comments on nonlinear wave equations as models for elementary particles, J. Math. Phys. **5**, 1252 (1964).

[5] T. H. R. Skyrme, A Nonlinear field theory, Proc. Roy. Soc. Lon. **260**, 127 (1961).

[6] I. E. Dzyaloshinskii, A thermodynamic theory of weak ferromagnetism of antiferromagnetics, J. Phys. Chem. Sol. **4**, 241 (1958).

[7] T. Moriya, Anisotropic superexchange interaction and weak ferromagnetism, Phys. Rev. **120**, 91 (1960).

[8] I. E. Dzyaloshinskii, Theory of helicoidal structures in antiferromagnets. I. Nonmetals, Zh. Eksp. Teor. Fiz. **46**, 1420 (1964) [Sov. Phys. JETP 19, 960 (1964)]; The theory of helicoidal structures in antiferromagnets. II. Metals, 47(1), 336 (1964) [Sov. Phys. JETP 20(1), 223 (1965)].

[9] A. N. Bogdanov and D. A. Yablonsky, Theormodynamically stable vortices in magnetically ordered crystals. Mixed state of magnetics, Zh. Eksp. Teor. Fiz. **95**, 178 (1989) [Sov. Phys. JETP **68**, 101 (1989)].

[10] A. Bogdanov and A. Hubert, Thermodynamically stable magnetic vortex states in magnetic crystals, J. Magn. Magn. Mater. **138**, 255 (1994); The stability of vortex-like structures in uniaxial ferromagnets, **195**, 182 (1999).

[11] A. N. Bogdanov and U. K. Rößler, Chiral Symmetry Breaking in Magnetic Thin Films and Multilayers, Phys. Rev. Lett. **87**, 037203 (2001).

[12] M. Bode, M. Heide, K. von Bergmann, P. Ferriani, S. Heinze, G. Bihlmayer, A. Kubetzka, O. Pietzsch, S. Blügel, and R. Wiesendanger, Chiral magnetic order at surfaces driven by inversion asymmetry, Nature (London) **447**, 190 (2007).

[13] D. C Wright and N. D. Mermin, Crystalline liquids: the blue phases, Rev. Mod. Phys. **61**, 385 (1989).

[14] J. P. Sethna, Frustration and Curvature: Glasses and the Cholesteric Blue Phase, Phys. Rev. Lett. **51**, 2198 (1983); Frustration, curvature, and defect lines in metallic glasses and the cholesteric blue phase, Phys. Rev. B **31**, 6278 (1985).

[15] P. J. Ackerman and I. I. Smalyukh, Diversity of Knot Solitons in Liquid Crystals Manifested by Linking of Preimages in Torons and Hopfions, Phys. Rev. X **7**, 011006 (2017).

[16] I. I. Smalyukh, Y. Lansac, N. Clark, and R. Trivedi, Three-dimensional structure and multistable optical switching of triple-twisted particle-like excitations in anisotropic fluids, Nat. Mater. **9**, 139 (2010).

[17] P. J. Ackerman and I. I. Smalyukh, Static three-dimensional topological solitons in fluid chiral ferromagnets and colloids, Nat. Mater. **16**, 426 (2016).

[18] A. O. Leonov and K. Inoue, Homogeneous and heterogeneous nucleation of skyrmions in thin layers of cubic helimagnets, Phys. Rev. B **98**, 054404 (2018).

[19] G. P. Müller, F. N. Rybakov, H. Jonsson, S. Blügel, and N. S. Kiselev, Coupled quasimonopoles in chiral magnets, Phys. Rev. B **101**, 184405 (2020).

[20] E. M. R. Tomasello, R. Zivieri, L. Torres, M. Carpentieri, and G. Finocchio, A strategy for the design of skyrmion racetrack memories, Sci. Rep. **4**, 6784 (2014).

[21] J. Müller, Magnetic skyrmions on a two-lane racetrack, New J. Phys. **19**, 025002 (2017).

[22] W. Kang, Y. Huang, C. Zheng, W. Lv, Na Lei, Y. Zhang, X. Zhang, Y. Zhou, and W. Zhao, Voltage controlled magnetic skyrmion motion for racetrack memory, Sci. Rep. **6**, 23164 (2016).

[23] A. Fert, V. Cros, and J. Sampaio, Skyrmions on the track, Nat. Nanotechnol. **8**, 152 (2013).

[24] P. J. Ackerman, T. Boyle, and I. I. Smalyukh, Squirming motion of baby skyrmions in nematic fluids, Nat. Commun. **8**, 673 (2017).

[25] D. Foster *et al.*, Two-dimensional skyrmion bags in liquid crystals and ferromagnets, Nat. Phys. **15**, 655 (2019).

[26] F. N. Rybakov, A. B. Borisov, and A. N. Bogdanov, Three-dimensional skyrmion states in thin films of cubic helimagnets, Phys. Rev. B **87**, 094424 (2013).

[27] A. O. Leonov, Y. Togawa, T. L. Monchesky, A. N. Bogdanov, J. Kishine, Y. Kousaka, M. Miyagawa, T. Koyama, J. Akimitsu, Ts. Koyama, K. Harada, S. Mori, D. McGrouther, R. Lamb, M. Krajnak, S. McVitie, R. L. Stamps, and K. Inoue, Chiral Surface Twists and Skyrmion Stability in Nanolayers of Cubic Helimagnets, Phys. Rev. Lett. **117**, 087202 (2016).

[28] D. Wolf, S. Schneider, U. K. Rößler, A. Kovacs, M. Schmidt, R. E. Dunin-Borkowski, B. Büchner, B. Rellinghaus, and A. Lubk, Unveiling the three-dimensional spin texture of skyrmion tubes, arXiv:2101.12630 (2021).

[29] S. Schneider, D. Wolf, M. J. Stolt, S. Jin, D. Pohl, B. Rellinghaus, M. Schmidt, B. Büchner, S. T. B. Goennenwein, K. Nielsch, and A. Lubk, Induction Mapping of the 3D-Modulated Spin Texture of Skyrmions in Thin Helimagnets, Phys. Rev. Lett. **120**, 217201 (2018).

[30] X. Z. Yu, Y. Onose, N. Kanazawa, J. H. Park, J. H. Han, Y. Matsui, N. Nagaosa, and Y. Tokura, Real-space observation of a two-dimensional skyrmion crystal, Nature **465**, 901 (2010).

[31] X. Z. Yu, N. Kanazawa, Y. Onose, K. Kimoto, W. Z. Zhang, S. Ishiwata, Y. Matsui, and Y. Tokura, Near room-temperature formation of a skyrmion crystal in thin-films of the helimagnet FeGe, Nat. Mater. **10**, 106 (2011).

[32] I. I. Smalyukh, Review: knots and other new topological effects in liquid crystals and colloids, Rep. Prog. Phys. **83**, 106601 (2020).

[33] A. O. Leonov, A. N. Bogdanov, and K. Inoue, Toggle-switch-like crossover between two types of isolated skyrmions within the conical phase of cubic helimagnets, Phys. Rev. B **98**, 060411(R) (2018).

[34] H. R. O. Sohn, S. M. Vlasov, V. M. Uzdin, A. O. Leonov, and I. I. Smalyukh, Real-space observation of skyrmion clusters with mutually orthogonal skyrmion tubes, Phys. Rev. B **100**, 104401 (2019).

[35] K. Kadowaki, K. Okuda, and M. Date, Magnetization and magnetoresistance of MnSi, J. Phys. Soc. Jpn **51**, 2433 (1982).

[36] S. Mühlbauer, B. Binz, F. Jonietz, C. Pfleiderer, A. Rosch, A. Neubauer, R. Georgii, and P. Böni, Skyrmion lattice in a chiral magnet, Science **323**, 915 (2009).

[37] A. Chacon, L. Heinen, M. Halder, A. Bauer, W. Simeth, S. Muehlbauer, H. Berger, M. Garst, A. Rosch, and C. Pfleiderer, Observation of two independent skyrmion phases in a chiral magnetic material, Nat. Phys. **14**, 936 (2018).

[38] L. J. Bannenberg, H. Wilhelm, R. Cubitt, A. Labh, M. Schmidt, E. Lelievre-Berna, C. Pappas, M. Mostovoy, and A. O. Leonov, Multiple low-temperature skyrmionic states in a bulk chiral magnet, NPJ Quantum Mater. **4**, 11 (2019).

[39] S. M. Vlasov, V. M. Uzdin, and A. O. Leonov, Skyrmion flop transition and congregation of mutually orthogonal skyrmions in cubic mag-nets, J. Phys.: Cond. Matt. **32**, 185801 (2020).

[40] N. Nagaosa and Y. Tokura, Topological properties and dynamics of magnetic skyrmions, Nat. Nanotechnol. **8**, 899 (2013).

[41] C. Back *et al.*, The 2020 skyrmionics roadmap, J. Phys. D: Appl. Phys. **53**, 363001 (2020).

[42] U. K. Rößler, A. Leonov, and A. N. Bogdanov, Skyrmionic textures in chiral magnets, J. Phys.: Conf. Series **200**, 022029 (2010); Chiral skyrmionic matter in non-centrosymmetric magnets, **303**, 012105 (2011).

[43] A. P. Levanyuk and D. G. Sannikov, Theory of phase transitions in ferroelectrics accompanied by the formation of a superstructure whose period is not equal to a multiple of the initial period, Fiz. Tverd. Tela **18**, 1927 (1976) [Sov. Phys.-Sol. State, **18**, 245 (1976)]; Thermodynamic theory of phase transitions accompanied by the formation of the noncommensurate superstructure in $NaNO_2$, Sov Physics Solid State **18**, 1122 (1976).

[44] Yu. A. Izyumov, Modulated, or long-periodic, magnetic structures of crystals, Sov. Phys. Usp. **27**, 845 (1984).

[45] H. Z. Cummins, Experimental studies of structurally incommensurate crystal phases, Phys. Rep. **185**, 211 (1990).

[46] A. N. Bogdanov, U. K. Rößler, M. Wolf, and K.-H. Müller, Magnetic structures and reorientation transitions in noncentrosymmetric uniaxial antiferromagnets, Phys. Rev. B **66**, 214410 (2002).

[47] P. Bak and M. H. Jensen, Theory of helical magnetic structures and phase transitions in MnSi and FeGe, J. Phys.C: Solid State Phys. **13**, L881 (1980).

[48] A. O. Leonov and I. Kezsmarki, textitAsymmetric isolated skyrmions in polar magnets with easy-plane anisotropy, Phys. Rev. B **96**, 014423 (2017).

[49] Y. Togawa, T. Koyama, K. Takayanagi, S. Mori, Y. Kousaka, J. Akimitsu, S. Nishihara, K. Inoue, A. S. Ovchinnikov, and J. Kishine, Chiral Magnetic Soliton Lattice on a Chiral Helimagnet, Phys. Rev. Lett. **108**, 107202 (2012).

[50] I. Kezsmarki, S. Bordacs, P. Milde, E. Neuber, L. M. Eng, J. S. White, H. M. Ronnow, C. D. Dewhurst, M. Mochizuki, K. Yanai, H. Nakamura, D. Ehlers, V. Tsurkan, and A. Loidl, Neel-type skyrmion lattice with confined orientation in the polar magnetic semiconductor GaV_4S_8, Nat. Mater. **14**, 1116 (2015).

[51] K. Geirhos, B. Gross, B. G. Szigeti, A. Mehlin, S. Philipp, J. S. White, R. Cubitt, S. Wid-mann, S. Ghara, P. Lunkenheimer, V. Tsurkan, E. Neuber, D. Ivaneyko, P. Milde, L. M. Eng, A. O. Leonov, S. Bordacs, M. Poggio, and I. Kezsmarki, Macroscopic manifestation of domain-wall magnetism and magnetoelectric effect in a Neel-type skyrmion host, npj (Nat. Partner J.) Quantum Mat. **5**, 44 (2020).

[52] D. McGrouther, R. J. Lamb, M. Krajnak, S. McFadzean, S. McVitie, R. L. Stamps, A. O. Leonov, A. N. Bogdanov, and Y. Togawa, Internal structure of hexagonal skyrmion lattices in cubic helimagnets, New J. of Phys. **18**, 095004 (2016).

[53] M. T Birch, D. Cortés-Ortuño, L. A. Turnbull, M. N. Wilson, F. Groß, N. Träger, A. Laurenson, N. Bukin, S. H. Moody, M. Weigand, G. Schütz, H. Popescu, R. Fan, P. Steadman, J. A. T. Verezhak, G. Balakrishnan, J. C. Loudon, A. C. Twitchett-Harrison, O. Hovorka, H. Fangohr, F. Y. Ogrin, J. Gräfe *et al.*, Real-space imaging of confined magnetic skyrmion tubes, Nat. Commun. **11**, 1726 (2020).

[54] M. T. Birch, D. Cortés-Ortuño, N. D. Khanh, S. Seki, A. Štefančič, G. Balakrishnan, Y. Tokura, and P. D. Hatton, Topological defect-mediated skyrmion annihilation in three dimensions, Communications Physics **4**, 175 (2021).

[55] A. O. Leonov, T. L. Monchesky, J. C. Loudon, and A. N. Bogdanov, Three-dimensional chiral skyrmions with attractive interparticle interactions, J. Phys.: Condens. Matter. **28**, 35LT01 (2016).

[56] A. O. Leonov, J. C. Loudon, and A. N. Bogdanov, Spintronics via non-axisymmetric skyrmions, Appl. Phys. Lett. **109**, 172404 (2016).

[57] H. Du, X. Zhao, F. N. Rybakov, A. B. Borisov, S. Wang, J. Tang, C. Jin, C. Wang, W. Wei, N. S. Kiselev, Y. Zhang, R. Che, S. Blügel, and M. Tian, Interaction of Individual Skyrmions in a Nanostructured Cubic Chiral Magnet, Phys. Rev. Lett. **120**, 197203 (2018).

[58] D. Capic, D. A. Garanin, and E. M. Chudnovsky, Skyrmion-skyrmion interaction in a magnetic film, J. Phys.: Cond. Matt. **32**, 415803 (2020).

[59] J. C. Loudon, A. O. Leonov, A. N. Bogdanov, M. C. Hatnean, and G. Balakrishnan, Direct observation of attractive skyrmions and skyrmion clusters in the cubic helimagnet Cu_2 $OSeO_3$, Phys. Rev. B **97**, 134403 (2018).

[60] A. O. Leonov, T. L. Monchesky, N. Romming, A. Kubetzka, A. N. Bogdanov, and R. Wiesendanger, The properties of isolated chiral skyrmions in thin magnetic films, New J. of Phys. **18**, 065003 (2016).

[61] J. Müller, J. Rajeswari, P. Huang, Y. Murooka, H. M. Ronnow, F. Carbone, and A. Rosch, Magnetic Skyrmions and Skyrmion Clusters in the Helical Phase of Cu_2 $OSeO_3$, Phys. Rev. Lett. **119**, 137201 (2017).

[62] A. B. Butenko, A. A. Leonov, U. K. Rößler, and A. N. Bogdanov, Stabilization of skyrmion textures by uniaxial distortions in noncentrosymmetric cubic helimagnets, Phys. Rev. B **82**, 052403 (2010).

[63] Y. Nii, T. Nakajima, A. Kikkawa, Y. Yamasaki, K. Ohishi, J. Suzuki, Y. Taguchi, T. Arima, Y. Tokura, and Y. Iwasa, Uniaxial stress control of skyrmion phase, Nat. Commun. **6**, 8539 (2015).

[64] A. Chacon, A. Bauer, T. Adams, F. Rucker, G. Brandl, R. Georgii, M. Garst, and C. Pfleiderer, Uniaxial Pressure Dependence of Magnetic Order in MnSi, Phys. Rev. Lett. **115**, 267202 (2015).

[65] Levatic, P. Popcevic, V. Surija, A. Kruchkov, H. Berger, A. Magrez, J. S. White, H. M. Ronnow, and I. Zivkovic, Dramatic pressure-driven enhancement of bulk skyrmion stability, Sci. Rep. **6**, 21347 (2016).

[66] A. O. Leonov, C. Pappas, and I. Kezsmarki, Field and anisotropy driven transformations of spin spirals in cubic skyrmion hosts, Phys. Rev. Research **2**, 043386 (2020).

[67] M. Preißinger, K. Karube, D. Ehlers, B. Szigeti, H.-A. Krug von Nidda, J. S. White, V. Ukleev, H. M. Ronnow, Y. Tokunaga, A. Kikkawa, Y. Tokura, Y. Taguchi, and I. Kezsmarki, Vital role of anisotropy in cubic chiral skyrmion hosts, npj Quantum Materials **6**, 65 (2021).

[68] M. T. Birch, S. H. Moody, M. N. Wilson, M. Crisanti, O. Bewley, A. Stefancic, G. Balakrishnan, R. Fan, P. Steadman, D. Alba Venero, R. Cubitt, and P. D. Hatton, Anisotropy-induced depinning in the Zn-substituted skyrmion host Cu_2 $OSeO_3$, Phys. Rev. B **102**, 104424 (2020).

[69] C. Pappas, E. Lelievre-Berna, P. Falus, P. M. Bentley, E. Moskvin, S. Grigoriev, P. Fouquet, and B. Farago, Chiral Paramagnetic Skyrmion-like Phase in MnSi, Phys. Rev. Lett. **102**, 197202 (2009).

[70] H. Wilhelm, M. Baenitz, M. Schmidt, U. K. Rößler, A. A. Leonov, and A. N. Bogdanov, Precursor Phenomena at the Magnetic Ordering of the Cubic Helimagnet FeGe, Phys. Rev. Lett. **107**, 127203 (2011).

[71] A. O. Leonov, U. K. Rößler, and M. Mostovoy, Target-skyrmions and skyrmion clusters in nanowires of chiral magnets, EPJ Web Conf. **75**, 05002 (2014).

[72] F. Zheng, H. Li, S. Wang, D. Song, C. Jin, W. Wei, A. Kovacs, J. Zang, M. Tian, Y. Zhang, H. Du, and R. E. Dunin-Borkowski, Direct Imaging of a Zero-Field Target Skyrmion and Its Polarity Switch in a Chiral Magnetic Nanodisk, Phys. Rev. Lett. **119**, 197205 (2017).

[73] D. Cortes-Ortuno, N. Romming, M. Beg, K. von Bergmann, A. Kubetzka, O. Hovorka, H. Fangohr, and R. Wiesendanger, Nanoscale magnetic skyrmions and target states in confined geometries, Phys. Rev. B **99**, 214408 (2019).

[74] X. Zhang, J. Xia, Y. Zhou, D. Wang, X. Liu, W. Zhao, and M. Ezawa, Control and manipulation of a magnetic skyrmionium in nanostructures, Phys. Rev. B **94**, 094420 (2016).

[75] A. O. Leonov and M. Mostovoy, Multiply periodic states and isolated skyrmions in an anisotropic frustrated magnet, Nat. Commun. **6**, 8275 (2015).

[76] X. Zhang, Y. Zhou, and M. Ezawa, High-topological-number magnetic skyrmions and topologically protected dissipative structure, Phys. Rev. B **93**, 024415 (2016).

[77] Y. A. Kharkov, O. P. Sushkov, and M. Mostovoy, Bound States of Skyrmions and Merons near the Lifshitz Point, Phys. Rev. Lett. **119**, 207201 (2017).

[78] P. Oswald and P. Pieranski, *Nematic and Cholesteric Liquid Crystals: Concepts and Physical Properties Illustrated by Experiments* (CRC Press, Boca Raton, FL, 2005).

[79] A. P. Ges, V. V. Fedotova, A. K. Bogush, and T. A. Gorbachevskaya, Spiral domains in single-crystal iron garnet films in static magnetic fields, JETP Lett. **52**, 476 (1990).

[80] G. S. Kandaurova, New phenomena in the low-frequency dynamics of magnetic domain ensembles, Phys. Usp. **45**, 1051 (2002).

[81] A. B. Borisov and F. N. Rybakov, Spiral structures in helicoidal magnets, JETP Lett. **96**, 521 (2012).

[82] R. Voinescu, J.-S. B. Tai, and I. I. Smalyukh, Hopf Solitons in Helical and Conical Backgrounds of Chiral Magnetic Solids, Phys. Rev. Lett **125**, 057201 (2020).

[83] M. Ezawa, Compact merons and skyrmions in thin chiral magnetic films, Phys. Rev. B **83**, 100408(R) (2011).